

WARM SECTOR TORNADOES WITHOUT DISCERNIBLE SURFACE BOUNDARIES AND WITH MINIMAL DEEP LAYER SHEA

Joshua M. Boustead* and Philip N. Schumacher
National Weather Service Sioux Falls, SD

1. INTRODUCTION

On 24 June 2003 an outbreak of tornadoes affected the states of Nebraska, Iowa, Minnesota and South Dakota. Of the 100 tornadoes that occurred, 91 of the tornadoes were weak (F1 or less; Fujita 1971), the strongest tornado, rated F4, destroyed the town of Manchester, South Dakota. The state of South Dakota recorded a record 67 tornadoes, of which 64 occurred in the county warning area (CWA) of the National Weather Service (NWS) in Sioux Falls, SD (Fig. 1).

This outbreak is an example of an extreme local tornado outbreak. All of the tornadoes occurred within a 6 hour period from near 2200 UTC 24 June through 0400 UTC 25 June. This significant of a tornado outbreak not only presents a danger to life and property in the local area, but also presents workload and resources problem to the NWS both staffing during the event and during post-event survey and documentation.

In addition to the number of tornadoes in a short period of time, the environment in which the parent supercells developed varied across the FSD CWA. A significant number of the tornadoes reported on 24 June occurred with four cyclonic supercells that occurred in the warm sector. These supercells produced tornadoes in an environment that only weakly supported supercell potential. The NWS FSD CWA can be divided into 3 distinct environments during the 24 June outbreak (Fig. 2). Area #1 favored the more classic and persistent supercells, while area #2 supported multi-celled thunderstorms and high precipitation supercells, and was the source region of an intense squall line which became dominate later in the event. The environment in area #3 produced a number of cyclonic and anticyclone warm-sector supercells with numerous tornadoes. This note will compare the mode of convection and resultant severe weather in areas of #1 and #3.

2. Synoptic Environment

The large-scale environment at 1200 UTC 24 June indicated a long-wave trough over the western United States (Fig. 3). A number of short-wave troughs were embedded in the broad southwest flow across the central and western United States. The short-wave located from Wyoming to northeast Colorado at 1200 UTC lifted into southern South Dakota by 0000 UTC 25 June (Fig. 4). This short-wave was responsible for

spreading large-scale adiabatic vertical motion across eastern South Dakota and Nebraska during the afternoon hours of 24 June.

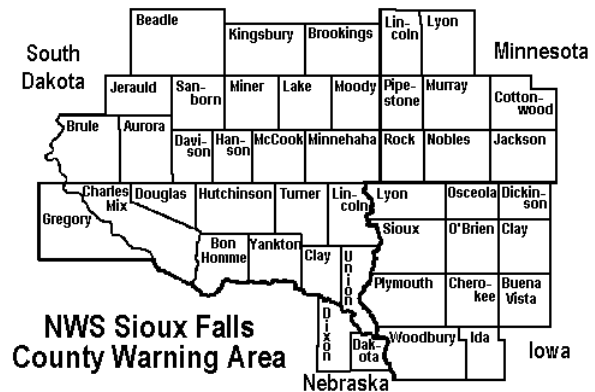


Figure 1. County warning area of the National Weather Service in Sioux Falls, SD.

The atmosphere across eastern South Dakota and Nebraska became extremely unstable during the afternoon with good insolation and steep 700 to 500 hPa lapse rates of $7.5 \text{ }^\circ\text{C km}^{-1}$. Observed upper air soundings from both Omaha, Nebraska (OAX) and Aberdeen, South Dakota (ABR) indicated these steep lapse rates at both 1800 UTC 24 June and 0000 UTC 25 June (Fig. 5). ABR is located on the cool side of the synoptic surface boundary and is stable when lifting a 100 hPa mixed-layer (ML) parcel. However, with steep mid tropospheric lapse rates, there is 2000 J kg^{-1} of convective available potential energy (CAPE) with parcels

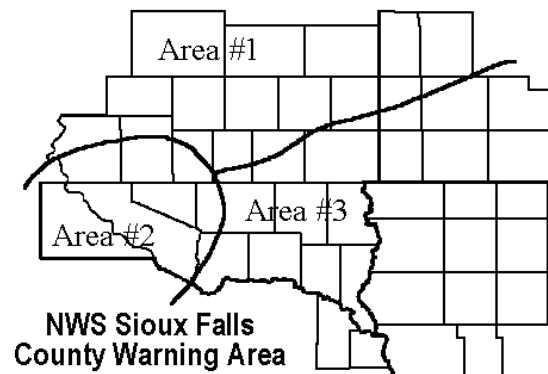
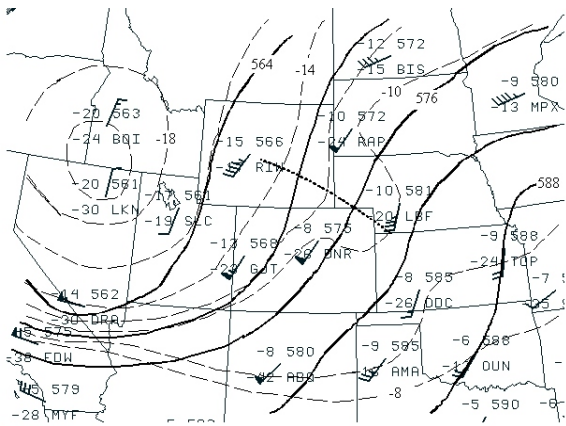


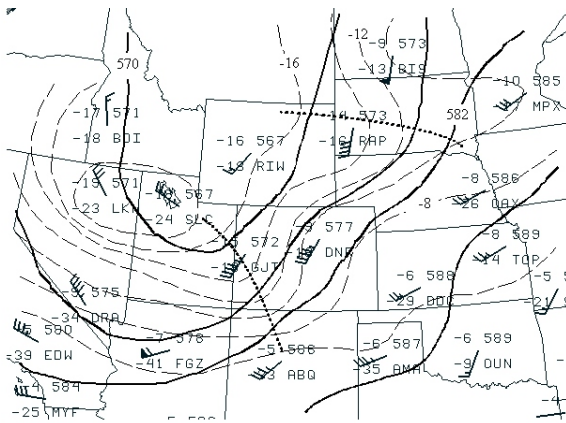
Figure 2. Environmental areas of the FSD CWA during the 24 June tornado outbreak.

*Corresponding author address: 26 Weather Lane, Sioux Falls, SD 57104; 605-330-4244; email: joshBoustead@noaa.gov



030624/1200

Figure 3. 1200 UTC 24 June subjective 500 hPa analysis. Thick dark contours are heights ever 30 meters and labeled ever 60 meters. Short-dashed light lines are temperatures in °C ever 2 °C and labeled ever 4 °C. Dotted line indicates position of short-wave trough.



030625/0000

Figure 4. Same as figure 3 for 0000 UTC 25 June.

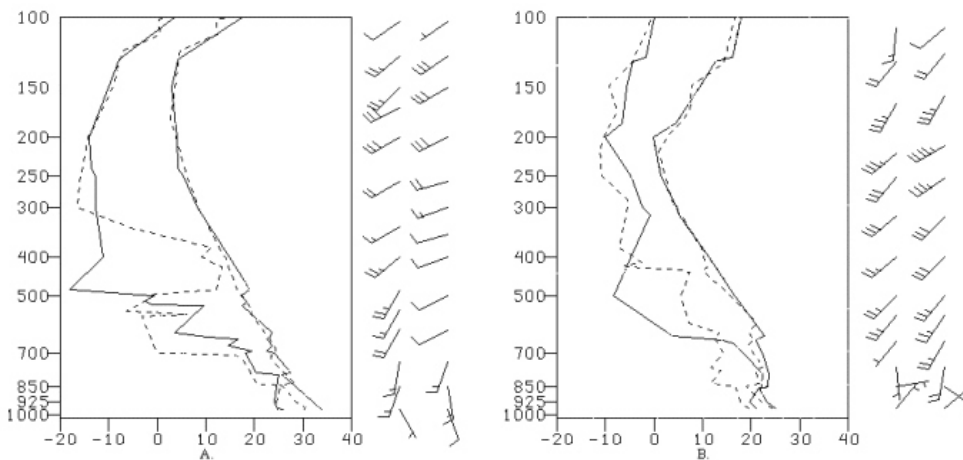


Figure 5. Observed upper air soundings from Omaha, NE (A) and Aberdeen, SD (B). Short-dashed line is the 1800 UTC 24 June sounding and the thick dark line is the 0000 UTC 25 June sounding. Wind position one is 1800 UTC and wind position two is 0000 UTC.

lifted from 800 hPa at 0000 UTC. The OAX sounding is located within the warm sector of the surface cyclone. The amount of boundary layer deepening and lift from 1800 to 0000 UTC is visible when the soundings are compared. A parcel would lift without restraint to the level of free convection (LFC) with a surface temperature and dewpoint of 33 °C and 21 °C respectively. These surface conditions would yield a MLCAPE of 4300 J kg⁻¹ with near 0 J kg⁻¹ of convective inhibition (CIN). Thus the warm sector ahead of the surface cyclone and upper-level disturbance was unstable and only weakly capped as the temperatures across Nebraska and eastern South Dakota climbed into the 30 to 33 °C range with surface dewpoint temperatures around 24 °C.

Also visible in the observed soundings is the increased gradient in deep-layer shear from ABR to OAX. At OAX the boundary-layer (500 m) to 6 km (hereafter BL-6km) shear increased from 16 ms⁻¹ at 1800 UTC 24 June to 18 ms⁻¹ at 0000 UTC 25 June. The shear at ABR increased from 30 ms⁻¹ at 1800 UTC to 37 ms⁻¹ at 0000 UTC. This increased gradient was a response to a short-wave ridge that moved over eastern Nebraska during the afternoon, while the Wyoming shortwave moved into South Dakota. Using the Neligh, Nebraska (NLG) wind profiler, the velocity azimuthal display (VAD) wind profilers from North Platte, Nebraska (LBF) and FSD weather surveillance radar (WSR) 1988-Doppler (WSR-88D), as well as the 0000 UTC 25 June RUC analysis (not shown), the eastward extent of the 15 ms⁻¹ BL-6km isoshear can be plotted. The 15 ms⁻¹ isoshear extended from northeast Nebraska into southwest Minnesota (Fig. 6), which created a significant gradient in expected storm type and longevity across the FSD CWA. This gradient was responsible for the 3 modes of convection observed across the FSD CWA on 24 June.

3. Mesoscale Environment

A true mesoscale (Orlanski 1975) analysis cannot be conducted due to an average of 95 km space between observation points across the FSD CWA. Nevertheless, with the help of satellite and radar data (not shown), a near mesoscale analysis can be performed. In addition, with the use of observed upper air soundings, the wind profiler network, VAD wind profilers, and model analysis

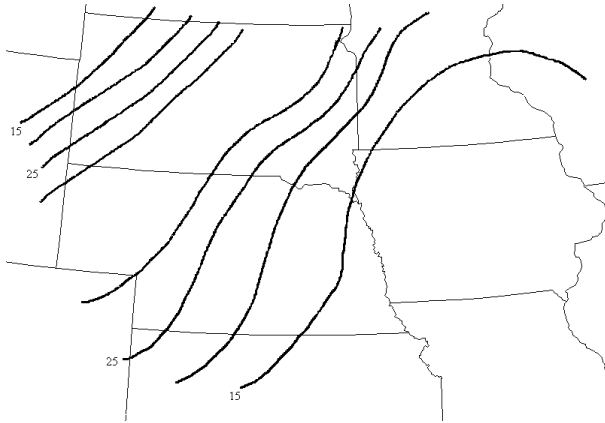


Figure 6. 0000 UTC 25 June subjective BL-6km isoshear analysis. Contours are in ms^{-1} ever 5 ms^{-1} and labeled ever 10 ms^{-1} .

fields, hodographs can be constructed to represent the 3 different sectors across the FSD CWA.

The 1800 UTC 24 June subjective surface analysis is presented in figure 7. The synoptic warm front extended from a surface low in Nebraska across southeast South Dakota into southwest Minnesota. A secondary warm front induced from

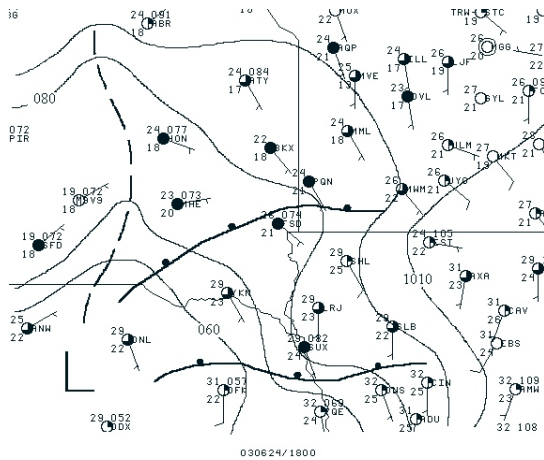


Figure 7. 1800 UTC subjective surface analysis. Thick contour are isobars measured ever 1 hPa and labeled ever 2 hPa. Station plots temperature and dewpoint are in $^{\circ}\text{C}$. Wind barbs are in ms^{-1} with a short-barb being 5 ms^{-1} and a long barb being 10 ms^{-1} .

nocturnal convection extended across eastern Nebraska and western Iowa. By 2100 UTC (Fig. 8) the surface low had lifted into southeast South Dakota in response to the advance of the Wyoming short-wave. The warm sector had quickly recovered from the nocturnal convection with the southern warm front losing definition in the deep warm air advection (WAA) regime. At 0000 UTC 25 June the surface low was located over southeast South Dakota with the synoptic warm front extending from the low into central Minnesota (Fig. 9). The majority of the FSD CWA was now in the warm sector of the surface cyclone. The evolution of the surface analyses

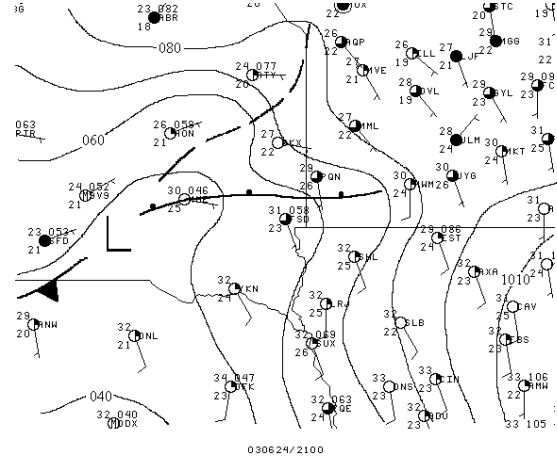


Figure 8. Same as figure 7 for 2100 UTC 24 June.

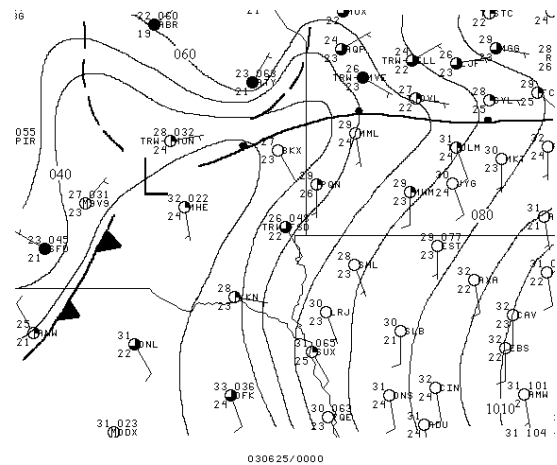


Figure 9. Same as figure 7 for 0000 UTC 25 June.

indicated that as the Wyoming short-wave approached, WAA allowed for quick recovery of the warm sector. By 2100 UTC there appears to be a lack of discernible surface boundaries across the warm-sector, and this is also supported by radar and satellite imagery (not shown).

Figure 10 is a hodograph constructed in area #1 at 0000 UTC 24 June. This hodograph indicated a number of characteristics that have been identified as favorable for potential supercell and tornadogenesis. Rasmussen and Blanchard (1998) published a baseline climatology of severe weather parameters which can help forecasters anticipate the mode of convection and potential for tornadoes. The BL-6km shear in figure 10 indicates a strong potential for supercell thunderstorms. Later research by Rasmussen (2003) indicated that storm-relative helicity (SRH; Davies-Jones et al. 1990) integrated in the lowest 1 km is a good indicator of tornadic supercells. The SRH computed for the 0 to 1 km layer in area #1 was $140 \text{ m}^2\text{s}^{-2}$, which is above the 50th percentile found in the Rasmussen study. The combination of strong deep-layer shear, strong low-level SRH and sufficient instability led to the development of classic supercells and associated strong tornadoes in this area.

Figure 11 is the hodograph from area #2 of the FSD CWA. In this area, four cyclonic supercells were responsible for 31 of the total tornadoes with two of these tornadoes reaching F2 strength. BL-6km shear for this sounding is 16 ms^{-1} , with a significant portion of this shear associated with mid-level directional shear. Thunderstorms that developed in this region were able to develop a mid-level mesocyclone but were relatively short-lived with no supercell lasting longer than 1 hour.

Although the BL-6km shear indicates some supercell potential, there is a lack of directional shear in the lowest 1 km of the hodograph. SRH integrated in the lowest 1 km computed with storm motion is only $9 \text{ m}^2\text{s}^{-2}$. This is well below the 25th percentile that Rasmussen indicated in 2003. As indicated in the subjective surface analysis, there also appeared to be a lack of discernable surface boundaries with which thunderstorms could interact to increase the low-level SRH. This has been shown to be helpful in situations there is

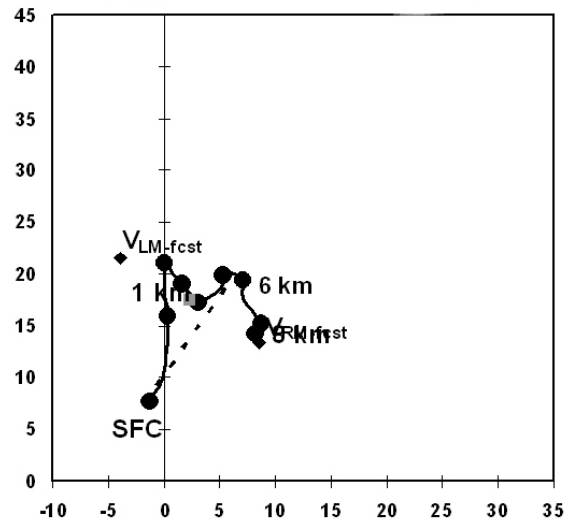


Figure 11. Same as figure 10 for area #3 of the FSD CWA.

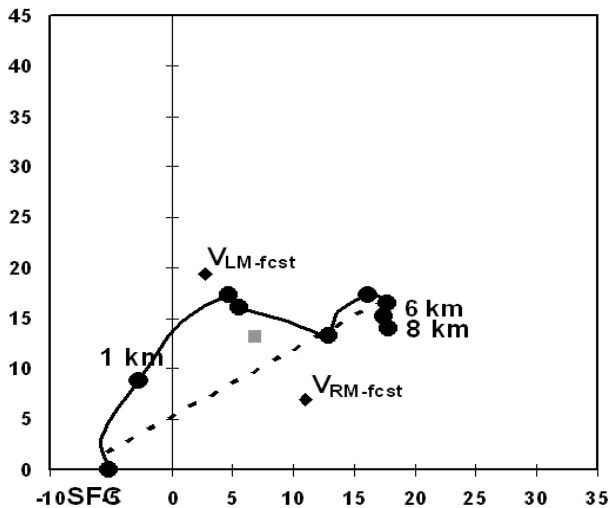


Figure 10. 0000 UTC hodograph from area #1 of the FSD CWA. Wind is in ms^{-1} .

a lack of very strong ambient shear (Markowski et al. 1998). It appears these short-lived supercells were able to produce a significant number of tornadoes, with two being in the strong category (F2), by a combination of significant speed shear in the lowest 2 km and a significant amount of instability in the lowest 3 km. The amount of speed shear in the lowest 2 km of the hodograph in area #3 is 13 ms^{-1} . The quantity of speed shear significantly increases after 0000 UTC 25 June as the nocturnal plains low-level jet developed. A RUC analysis sounding at 0000 UTC from area #2 indicates near 135 J kg^{-1} of CAPE, which is above the 75th percentile found in the Rasmussen (1998) study to be supportive of tornadic supercells. The combination of the thunderstorms remaining surface-based as the low-level jet increased and the degree of lower level instability led to the ability of the supercells in this area to produce tornadoes, even with a lack of discernable low-level boundaries.

4. Conclusion

The tornado outbreak on 24 June 2004 is important for a number of reasons. First, this is a case of an extreme local outbreak with a significant number of tornadoes. This amount of severe weather in a local WFO CWA can be difficult to handle during and after the event. Second, there appears to be a large number of tornadoes that occurred in the warm sector with a lack of strong BL-6km shear and no discernable surface boundaries. Finally, this presents a significant forecast challenge to local and national forecasters to anticipate such an event.

On 24 June 2004 supercells developed in an environment that was not supportive of long-lived supercells with strong

tornadoes. These supercells produced a significant amount of the tornadoes on 24 June, with two of the tornadoes reaching F2 strength. The anticipation of environments that can produce this type of supercell is not well understood. There appeared to be sufficient lower level instability and speed shear in the lowest 3 and 2 km respectively to overcome the lack of significant SRH in the 0 to 1 km layer. Thus the short-lived supercells also were able to produce tornadoes without discernable surface boundaries. Thus in the warm season, when extreme instability is expected, it is important to also anticipate if warm sector thunderstorms will be able to ingest surface parcels once insolation decreases and the nocturnal low-level jet increases and the low-level speed shear increases significantly.

During the 24 June event there were 3 distinct environments in which thunderstorms were developing in the FSD CWA. Each individual warning forecaster needed to be aware of how the environment in their area is evolving, and how this affects the mode of convection and resultant severe weather that could be expected. This

emphasizes the need for detailed mesoscale analysis during convective events.

5. References

Davies-Jones, R.P., D. Burgess, and M. Foster,

1990: Test of helicity as a tornado forecast parameter. Preprints, *16th Conf. On Severe Local Storms*, Kananaskis Park, AB, Canada, Amer. Meteor. Soc., 588-592.

Fujita, T. T., 1971: Proposed characterization of tornadoes and hurricanes by area and intensity. Satellite and Meteor. Res. Project. Department of Geophy. Sci., The University of Chicago., 42.

Orlanski, I., 1975: A rational subdivision of scale for atmospheric processes. *Bull. Amer. Meteor. Soc.*, **56**, 527-530.

Rasmussen, E. A., Blanchard, D. O., 1998: A baseline climatology of sounding-derived supercell and tornado forecast parameters. *Wea. Forecasting*, **13**, 1148-1164.

_____, 2003: Refined supercell and tornado forecast parameters. *Wea. Forecasting*, **5**, 530-535.